Acta Crystallographica Section C
**Crystal Structure Communications**
ISSN 0108-2701

# Herringbone array of hydrogen-bonded ribbons in 2-ethoxybenzamide from high-resolution X-ray powder diffraction

**Silvina Pagola[a]* and Peter W. Stephens[b]**

[a]Department of Applied Science, College of William and Mary, Williamsburg, VA 23187, USA, and Applied Research Center, 12050 Jefferson Avenue, Newport News, VA 23606, USA, and [b]Department of Physics and Astronomy, SUNY at Stony Brook, Stony Brook, NY 11794-3800, USA
Correspondence e-mail: spagol@wm.edu

Received 8 September 2009
Accepted 6 October 2009
Online 17 October 2009

In 2-ethoxybenzamide, $C_9H_{11}NO_2$, the amide substituents are linked into centrosymmetric head-to-head hydrogen-bonded dimers. Additional hydrogen bonds between adjacent dimers give rise to ribbon-like packing motifs, which extend along the *c* axis and possess a third dimension caused by twisting of the 2-ethoxyphenyl substituent with respect to the hydrogen-bonded amide groups. The ribbons are arranged in a T-shaped herringbone pattern and cohesion between them is achieved by van der Waals forces.

## Comment

2-Ethoxybenzamide, (I), also called ethenzamide, is a compound with pharmaceutical applications as an analgesic and antipyretic (Kawano *et al.*, 1978; Darias *et al.*, 1992) in cold medications (Okamoto *et al.*, 2005). Besides its medicinal use, it is interesting from the crystal engineering point of view for the analysis of the usual packing modes of benzamides, which often involve the formation of head-to-head hydrogen-bonded dimers (Braga *et al.*, 1999).

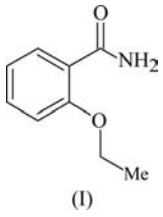


(I)

A search of the Cambridge Structural Database (CSD, Version 5.30; Allen, 2002) yielded 245 benzamide hits. Often having no, or rather small substituents, like benzamide, halobenzamides, *o*- and *m*-methylbenzamide and *o*-nitrobenzamide, the amide dimers arrange themselves into hydrogen-bonded ribbons using the remaining two H atoms of the two $-NH_2$ groups in each dimer and the unused oxygen lone pairs of the two carbonyl groups. In almost all cases, these ribbons run parallel to a cell axis with a dimension of about 5 Å (exceptionally 10 or 15 Å), given approximately by the projections of the donor–acceptor hydrogen-bond distances between dimers, plus the intramolecular amide N···O distance, on to the corresponding lattice direction. Occasionally, the hydrogen-bonded amide groups are not coplanar, forming the core of a 'ribbon', but rather in zigzag orientations, and the hydrogen-bonded packing motif produced forms the core of a flat object similar to a sheet, *e.g.* in *m*-chlorobenzamide (Hattori *et al.*, 1975). Only exceptionally does the packing not involve hydrogen-bonded dimers, but rather a hydrogen-bonded chain, *e.g.* in *p*-nitrobenzamide (Jones *et al.*, 2002) and *m*-bromobenzamide (Kato *et al.*, 1967). Occasionally, the dimers are isolated, *e.g.* in *p*-chlorobenzamide (Hayashi *et al.*, 1980); other examples with isolated dimers include cases with rather bulky substituents (Aakeroy *et al.*, 2007), in chlathrates (Reddy *et al.*, 2002) and in coordination compounds (Aakeroy *et al.*, 2005). More complex hydrogen-bonding arrangements form if additional hydrogen-bonding donors or acceptors are present, *e.g.* in *o*-acetamidobenzamide (Errede *et al.*, 1981).

It is interesting to note that the parent compound, benzamide, shows three polymorphic forms. This polymorphism was first reported by Wöhler & von Liebig (1832), who reported the existence of two polymorphic forms. The crystal structure of the thermodynamically stable form I was solved in 1959 (Penfold & White, 1959), and form II was solved in 2005 (Bladgen *et al.*, 2005; David *et al.*, 2005) from synchrotron X-ray powder diffraction data. In addition, the conversion of form II to form I was reported. The structure of form III was reported in 2007 (Thun *et al.*, 2007). In all structures, the benzamide molecules form head-to-head hydrogen-bonded dimers, which are also arranged in ribbons as described above, extending along the shortest axis of their unit cells (around 5 Å) but differently packed (Thun *et al.*, 2007). The three forms present shifted $\pi$–$\pi$ stacks and T-shaped interactions. In

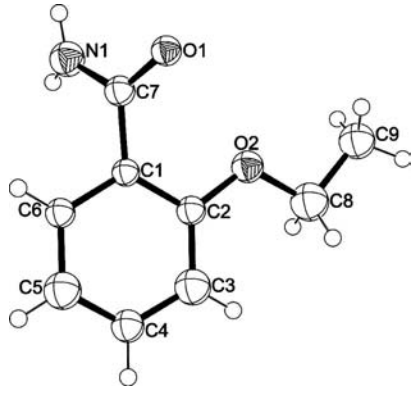


**Figure 1**
The molecular structure of (I), showing the labeling scheme used and the isotropic displacement parameters determined from the powder diffraction experiment at 50% probability level. H atoms are shown as small spheres of arbitrary radii.

 doi:10.1107/S0108270109040803  

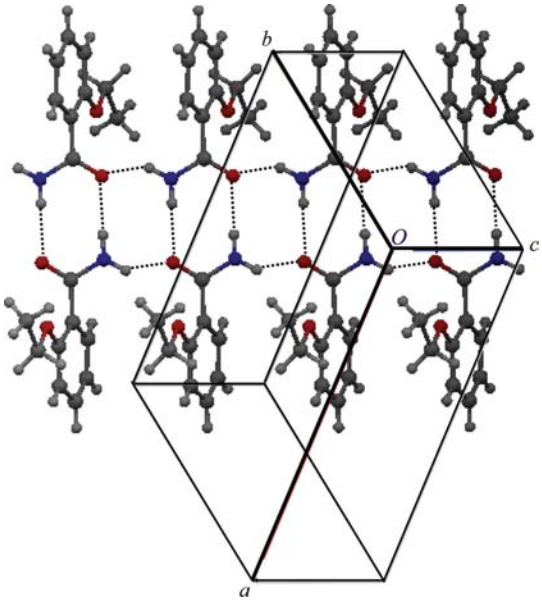


**Figure 2**
The amide hydrogen-bonding pattern (dashed lines) forming a ribbon-like packing motif in (I).

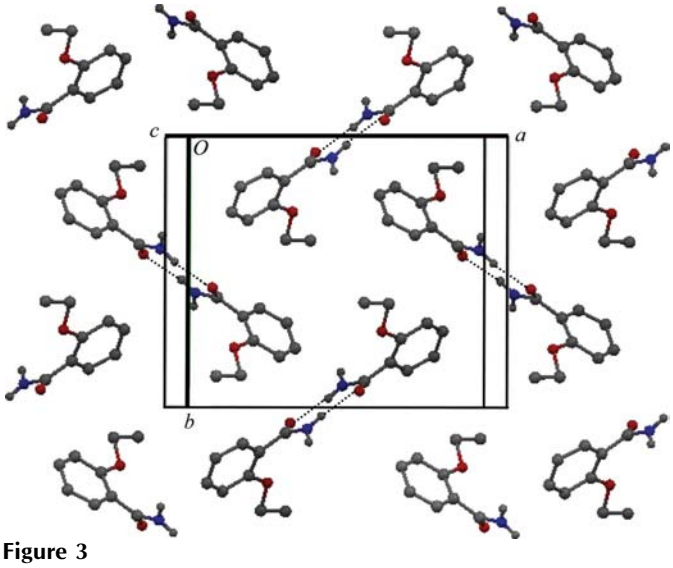


**Figure 3**
The herringbone array of hydrogen-bonded ribbons in (I), viewed approximately along [001]. H atoms not involved in hydrogen bonds have been omitted for clarity.

form II, the two molecules in the dimer are not related by inversion symmetry and considerable disorder is present in one of the molecules (Bladgen *et al.*, 2005; David *et al.*, 2005).

This work reports the crystal structure of 2-ethoxybenzamide, (I), obtained from its room-temperature high-resolution X-ray powder diffraction pattern. Bond distances and angles in (I) are as expected from the chemical bonding. Fig. 1 shows the molecular structure, the refined isotropic displacement parameters and the labelling scheme used.

The crystal structure of (I) is composed of centrosymmetric hydrogen-bonded amide dimers, located around the inversion centres at ($\frac{1}{2}$, 0, 0) and (0, $\frac{1}{2}$, $\frac{1}{2}$). Lattice translations generate two ribbon-like packing motifs, oriented differently and both

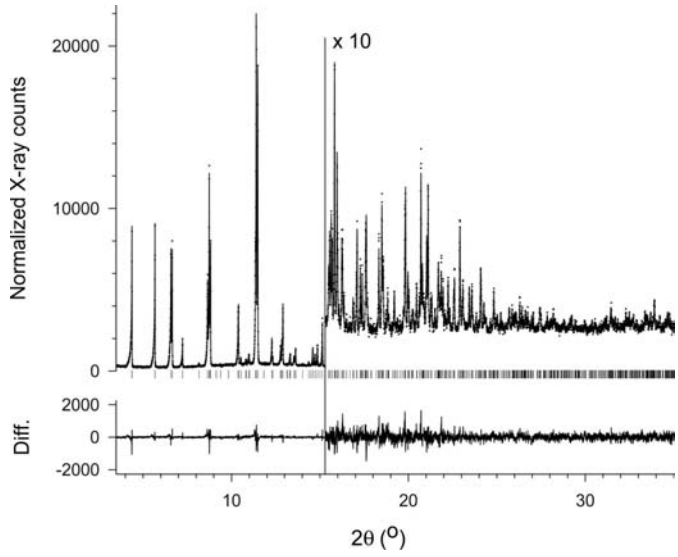


**Figure 4**
Rietveld refinement of the powder diffraction pattern of (I). Observed intensities are represented with dots, the calculated profile is shown with a solid line and the difference plot is at the bottom. Tick marks represent allowed peak positions.

extending along the *c* axis, of 5.05009 (6) Å, wherein the dimers are connected into ribbons by additional hydrogen bonds formed between the carbonyl O atom and the $-NH_2$ H atoms of adjacent amide groups, in a nearly coplanar array of amide C, N and O atoms. The hydrogen-bonded array and the ribbon-like packing motif are shown in Fig. 2. Hydrogen-bonding parameters are summarized in Table 1.

Cohesion between the ribbons in the crystal structure of (I) is achieved by van der Waals forces. The packing of the ribbons to extend the structure perpendicular to the *c* axis can be described as a T-shaped arrangement, wherein the 'edges' of one ribbon point to the 'planes' of adjacent ribbons, forming the herringbone array shown in Fig. 3.

Regarding the molecular conformation of (I) in the solid state, the ethoxy substituent is almost coplanar with the benzene ring, forming an angle of 8.2 (11)° (H-atom positions excluded), whereas the amide–benzene dihedral angle is 50.4 (14)°. This latter feature gives the ribbon a bounded third dimension, since the two aromatic rings in each dimer protrude at this angle from the plane of the amide group, with the 2-ethoxy substituents pointing in opposite directions (Fig. 2). It can be noted that the ribbons in form I of benzamide have a lesser three-dimensional character, since the angle between the amide and benzene groups is 26° (Penfold & White, 1959). Similar considerations apply to forms II and III.

Similar packing in $P2_1/a$, with a shortest axis of around 5 Å, was found in *o*-nitrobenzamide (Fujimori *et al.*, 1972).

## Experimental

A powder sample of (I) was obtained from Sigma–Aldrich and used as received. The crystallites had a needle-like habit, with the longest axis in the range 50–140 µm, as seen under an optical microscope.

*Crystal data*

$C_9H_{11}NO_2$
$M_r$ = 165.19
Monoclinic, $P2_1/n$
$a$ = 14.2141 (2) Å
$b$ = 12.0446 (1) Å
$c$ = 5.05009 (6) Å
$\beta$ = 96.5811 (8)°
$V$ = 858.89 (2) Å$^3$
$Z$ = 4
Synchrotron radiation
$\lambda$ = 0.69847 Å
$\mu$ = 0.11 mm$^{-1}$
$T$ = 298 K
Specimen shape: cylinder
8 × 1.5 × 1.5 mm
Specimen prepared at 101 kPa
Specimen prepared at 298 K
Particle morphology: needles (fine powder), white

*Data collection*

Huber adapted diffractometer
Specimen mounting: glass capillary
Specimen mounted in transmission mode
Scan method: step
Absorption correction: none
$2\theta_{min}$ = 1.0, $2\theta_{max}$ = 35.0°
Increment in $2\theta$ = 0.005°

*Refinement*

$R_p$ = 0.053
$R_{wp}$ = 0.063
$R_{exp}$ = 0.046
$R_B$ = 0.055
$S$ = 1.45
Wavelength of incident radiation: 0.69847 Å
Excluded region(s): 1–3.5° (diffraction peaks not present)
Profile function: pseudo-Voight (Thompson *et al.*, 1987) with asymmetry correction (Finger *et al.*, 1994)
578 reflections
96 parameters
60 restraints
H-atom parameters constrained
Preferred orientation correction: none

The powder diffraction pattern was indexed without impurity peaks using the program *DICVOL04* (Boultif & Louër, 2004) to a monoclinic lattice with $a$ = 14.2227 Å, $b$ = 12.0525 Å, $c$ = 5.0527 Å, $\beta$ = 96.552°, $V$ = 860.47 Å$^3$ and $M_{20}$ = 35.7. A Le Bail fit (Le Bail *et al.*, 1988) was carried out using the program *GSAS* (Larson & Von Dreele, 2004) and confirmed the lattice found. The Le Bail agreement factors are $R_{wp}$ = 0.0553 and $\chi^2$ = 1.6. The space group $P2_1/n$ was determined from the observation of the systematic absences and $Z$ was estimated as 4 from the estimated density (around 1.3 Mg m$^{-3}$). The molecular geometry used was optimized using the program *MOPAC2009* (Stewart, 2009).

The crystal structure was solved using the simulated annealing global optimization algorithm (Kirkpatrick *et al.*, 1983) implemented in the computer code *PSSP* (Powder Structure Solution Program; P. W. Stephens & S. Pagola; program available on request), using the correlated integrated intensities of the first 53 Bragg reflections.

The atomic positions of the H atoms were calculated using *WinGX* (Farrugia, 1999). All atomic positions were refined using soft bond-length and bond-angle restraints. The isotropic displacement parameters of all non-H atoms were refined independently, whereas those of the H atoms were constrained to 1.2 times the value of the bonded non-H atom. At an intermediate Rietveld refinement stage, the identities of the amide O and N atoms were switched and the bond-distance restraints changed accordingly, in order to obtain all positive displacement parameters.

The following parameters were refined: scale factor, background coefficients, lattice parameters, $2\theta$ zero error, peak profile parameters, atomic coordinates and isotropic displacement parameters. The standard uncertainties of the atomic coordinates were corrected using the procedure described by Scott (1983). The final Rietveld refinement graph is shown in Fig. 4.

Data collection: X16C beamline software; cell refinement: *GSAS* (Larson & Von Dreele, 2004); data reduction: *GSAS*; program(s) used to solve structure: *PSSP* (Powder Structure Solution Program; P. W. Stephens & S. Pagola; program available on request); program(s) used to refine structure: *GSAS*; molecular graphics: *ORTEP-3 for Windows* (Farrugia, 1997) and *Mercury* (Version 2.2; Macrae *et al.*, 2006); software used to prepare material for publication: *publCIF* (Westrip, 2009).

**Table 1**
Hydrogen-bond geometry (Å, °).

| $D$—H···$A$ | $D$—H | H···$A$ | $D$···$A$ | $D$—H···$A$ |
|---|---|---|---|---|
| N1—H1$A$···O1$^{i}$ | 0.86 | 2.06 | 2.917 (16) | 171 |
| N1—H1$B$···O1$^{ii}$ | 0.86 | 2.37 | 2.860 (14) | 116 |

Symmetry codes: (i) $-x+1, -y+2, -z$; (ii) $x, y, z+1$.

Use of the National Synchrotron Light Source, Brookhaven National Laboratory, was supported by the US Department of Energy, Office of Science, Office of Basic Energy Sciences, under contract No. DE-AC02-98CH10886. SP gratefully acknowledges the ICDD GIA No. 08-04 and the Physics Department, College of William and Mary, for funding.

Supplementary data for this paper are available from the IUCr electronic archives (Reference: FA3207). Services for accessing these data are described at the back of the journal.

## References

Aakeroy, C. B., Desper, J., Smith, M. M. & Urbina, J. F. (2005). *Dalton Trans.* pp. 2462–2470.
Aakeroy, C. B., Scott, B. M. T. & Desper, J. (2007). *New J. Chem.* **31**, 2044–2051.
Allen, F. H. (2002). *Acta Cryst.* B**58**, 380–388.
Bladgen, N., Davey, R., Dent, G., Song, M., David, W. I. F., Pulham, C. R. & Shankland, K. (2005). *Cryst. Growth Des.* **5**, 2218–2224.
Boultif, A. & Louër, D. (2004). *J. Appl. Cryst.* **37**, 724–731.
Braga, D., Grepioni, G. & Orpen, A. G. (1999). *Crystal Engineering: from Molecules and Crystals to Materials. NATO Science Series*, Vol. 538. Dordrecht: Kluwer Academic Publishers.
Darias, V., Bravo, L., Abdallah, S. S., Sanchez, M. C. C., Exposito-Orta, M. A., Lissavetsky, J. & Manzanares, J. (1992). *Arch. Pharm.* **325**, 83–87.
David, W. I. F., Shankland, K., Pulham, C. R., Bladgen, N., Davey, R. J. & Song, M. (2005). *Angew. Chem. Int. Ed.* **43**, 7032–7035.
Errede, L. A., Etter, M. C., Williams, R. C. & Darnauer, S. M. (1981). *J. Chem. Soc. Perkin Trans. 2*, pp. 233–238.
Farrugia, L. J. (1997). *J. Appl. Cryst.* **30**, 565.
Farrugia, L. J. (1999). *J. Appl. Cryst.* **32**, 837–838.
Finger, L. W., Cox, D. E. & Jephcoat, A. P. (1994). *J. Appl. Cryst.* **27**, 892–900.
Fujimori, K., Tsukihara, T., Katsube, Y. & Yamamoto, J. (1972). *Bull. Chem. Soc. Jpn*, **45**, 1564–1565.
Hattori, S., Taniguchi, T. & Sakurai, K. (1975). *Mem. Osaka Kyoiku Univ. III Nat. Sci. Appl. Sci.* **24**, 35–42.
Hayashi, T., Nakata, K., Takaki, Y. & Sakurai, K. (1980). *Bull. Chem. Soc. Jpn*, **53**, 801–802.
Jones, P. G., Thönnessen, H., Schmutzler, R. & Fischer, A. K. (2002). *Acta Cryst.* E**58**, o1436–o1438.
Kato, Y., Taniguchi, T., Takaki, Y. & Sakata, K. (1967). *Mem. Osaka Kyoiku Univ. III Nat. Sci. Appl. Sci.* **16**, 45–49.
Kawano, O., Sawabe, T., Misaki, N. & Fukawa, K. (1978). *Jpn J. Pharmacol.* **28**, 829–835.
Kirkpatrick, S., Gellat, C. D. Jr & Vecchi, M. P. (1983). *Science*, **220**, 671–680.
Larson, A. C. & Von Dreele, R. B. (2004). *GSAS*. Report LAUR 86-748. Los Alamos National Laboratory, New Mexico, USA.
Le Bail, A., Duroy, H. & Fourquet, J. L. (1988). *Mater. Res. Bull.* **23**, 447–452.

Macrae, C. F., Edgington, P. R., McCabe, P., Pidcock, E., Shields, G. P., Taylor, R., Towler, M. & van de Streek, J. (2006). *J. Appl. Cryst.* **39**, 453–457.
Okamoto, H., Nakajima, T., Ito, Y., Aketo, T., Shimada, K. & Yamato, S. (2005). *J. Pharm. Biomed. Anal.* **37**, 517–528.
Penfold, B. R. & White, J. C. B. (1959). *Acta Cryst.* **12**, 130–135.
Reddy, C. M., Nangia, A., Lam, C. & Mak, T. C. W. (2002). *CrystEngComm*, **4**, 323–325.
Scott, H. G. (1983). *J. Appl. Cryst.* **16**, 159–163.
Stewart, J. J. P. (2009). *MOPAC2009*. Stewart Computational Chemistry, Colorado Springs, Colorado, USA. http://openmopac.net/
Thompson, P., Cox, D. E. & Hastings, J. B. (1987). *J. Appl. Cryst.* **20**, 79–83.
Thun, J., Seyfarth, L., Senker, J., Dinnebier, R. & Breu, J. (2007). *Angew. Chem. Int. Ed.* **46**, 6729–6731.
Westrip, S. P. (2009). *publCIF*. http://journals.iucr.org/services/cif/publcif/
Wöhler, F. & von Liebig, J. (1832). *Ann. Pharm. (Lemgo, Ger.)*, **3**, 249–282.